

Nanosized particles in thin metal composite films and in gratings: modeling of their optical response

P. SHARLANDJIEV, D. NAZAROVA*

Central Laboratory of Optical Storage and Processing of Information, Bulgarian Academy of Sciences, P.O.Box 95, Sofia PS-1113, Bulgaria

Subwavelength diffraction gratings show enhanced optical transmission at certain wavelengths. These structures are intensively studied because of their potential for many novel applications. Recently, we have demonstrated by computer simulations that dielectric spheres randomly dispersed in metal host matrix have the same kind of resonant optical response. Herein, we present analysis of the extinction efficiency of a single dielectric sphere in Ag host matrix. Then, we examine the lower orders of the electric and magnetic modes, in order to find the poles that generate the morphology-dependent resonances. We also present analysis of the extinction efficiency of dielectric infinite circular cylinders in metal host matrix. Although the cylinders are randomly distributed in the metal film, their axes are assumed to be parallel to each other. Polarization effects are investigated and their dependence on the morphology of the dielectric particles is revealed. We discuss also the case when the dielectric cylinders are organized with certain periodicity in the metal film, thus forming a subwavelength diffraction grating. The features of the optical response of these structures strongly correlate.

(Received March 16, 2007; accepted June 27, 2007)

Keywords: Metal nanosized composite films, Subwavelength diffraction gratings

1. Introduction

Since the report of what the authors called rather inadequately ‘extraordinary transmission’ in metallic films with perforated arrays of holes [1] there is an intensive experimental and theoretical research on that phenomenon. Ebessen *et al.* [1] have observed an Enhanced Transmission (ET) of several orders of magnitude at certain wavelengths in such diffraction gratings. Later it was shown that perforations are not needed and TE can be observed in continuous diffractive or scattering structures [2, 3]. Recently we have demonstrated by computer simulations that dielectric spheres, randomly dispersed in metal host matrix have the same kind of optical response [4]. We have shown that the resonant peak spectral location is a sensitive function of the morphology of the dielectric particle – its shape, size and refractive index. Different mechanisms are proposed and discussed in an increasingly abounding literature, involving dynamic scattering assisted by Surface Plasmon Polaritons (SPPs), resonant transmission coupled to propagating modes, cavity mode resonances, etc [3]. The question of the dominant mechanism of ET in subwavelength gratings is still open.

Meanwhile a new branch of photonics has emerged – plasmonics, which has enormous potential for applications in optical computing and optical telecommunications [5 and references cited therein]. Plasmonics is based on excitation and manipulation of SPPs. SPP is a quasi particle but it is more readily understood as a light wave confined at a metal – dielectric interface and in interaction with the surface charges. Usually SPP is considered at planar surfaces. Herein we will focus on SPPs excited by metal volume roughness due to random or regular inhomogeneities.

In this work we present numeric simulations of the optical extinction of a single dielectric sphere in metal matrix and optical scattering of nanosized dielectric cylinders embedded in metal host matrix. They reveal ET and polarization effects depending on the morphology of the particles. These metal nanocomposite films may be considered as plasmonic ‘amorphous structures’ because they do not have long or short range symmetry and they do not obey wavevector conservation rules. We report also calculations on the optical response of certain diffraction gratings structures that have characteristics of plasmonic crystals. The optical behaviors of these periodic and random structures in visible and near IR spectral regions show enhanced resonant transmission although the physical origins are quite different.

2. Physical models

2.1. Homogeneous spherical particles

Our model consists of a homogeneous spherical particle with refractive index N_p between 1 and 1.74 embedded in a silver matrix. The Ag complex refractive index N_m is derived from [6] and interpolated with piecewise cubic Hermite spline technique. Sphere radius is varied between 5 and 150 nm.

Particle optical behavior is analyzed by the help of exact vector equations of scattering theory. Far-field scattered, internal and near-field external electromagnetic fields are calculated by the method of separation of variables. The scattered fields are estimated in terms of expansion coefficients, also called multipole electric $\{a_n\}$ and magnetic $\{b_n\}$ modes. They are functions of the particle size parameter $x = 2 \times \pi \times r \times N_m / \lambda$, where r is the sphere radius, N_m is the matrix (complex) refractive index,

and λ is the wavelength in vacuo. Expressions for the $\{a_n, b_n\}$ modes can be found in many books and references (see Ref. 7 and works there cited) and we will not quote them.

Resonances (sharp minima/maxima) in the internal and scattered fields are related to the poles of the expansion coefficients $\{a_n, b_n\}$. Our analysis is based on calculations of the extinction cross section per unit volume C_v which is well-defined physical quantity. It is known from standard Lorenz-Mie calculations that the wavelength dependence of C_v shows the existence of extremely narrow resonance structure. Spectral peak positions are related to the size of particle, its shape and refractive index, and the refractive index of the surrounding medium [7]. In absorbing host matrix C_v might have positive or negative values, as it follows from the optical theorem [8]. For non-absorbing matrix the extinction cross section may be presented as the sum of scattering and absorption cross sections. Many calculations and experimental results are treating this situation [9, 10]. However, in the case of an absorbing host this decomposition of extinction into scattering and absorption is not possible. In fact, negative C_v means an increase of the signal of a hypothetical detector, but the total extinction of the particle *and* host film is always positive [8].

Our numeric simulations relate the range of wavelengths where C_v has a negative minimum, to the location of the extraordinary transmission through the metal nanocomposite film. Thus, determination of the poles location is of major importance for identification of the spectral position of the extraordinary transmission. The presence of the particle affects the manner in which light is extinguished in the medium and leads to very sharp and high resonance peaks.

2.2. Nanosized cylinders

The physical model of the nanocomposite film that we consider is of a thin gold film of 110 nm thickness with embedded monodispersed infinite circular cylinders with radii 50 nm and refractive index of 1.5. Infinite cylinder means that its length is much longer than the diameter. Although the cylinders are randomly distributed in the film volume, their axes are assumed to be parallel to each other and perpendicular to the film normal. The metal film is surrounded by half spaces of refractive index 1.5. The complex dielectric function of the metal is taken from [6] interpolated. The dielectric particles are embedded at distances from the film surface that are less than the metal skin depth, which for Au is about 30 nm in the considered spectral range [9].

The scattering and extinction of the circular dielectric cylinder in absorption environment is analyzed by analogy with the previous paragraph and [11]. The propagating light at normal incidence impinges upon the composite film or grating structure, considered below.

The simplest periodic structure that we consider is a 1D subwavelength diffraction grating enclosed in half spaces (sub- and super-strates) of refractive index 1.5. The 100 nm thick gold grating has 500 nm period and is

formed by 100 nm square dielectric stripes (square cylinders with refractive index 1.5). At resonant condition SPPs are excited. We consider also the case when a homogeneous Au film is added at one of the grating surfaces, thus forming a 'unit cell' of a plasmonic crystal, formed by a succession of homogeneous metallic films and metallic gratings. This structure has infinite periodicity in the grating slab and finite periodicity in a perpendicular direction to the grating vector, due to the limited repetition of the 'unit cell'. In our model the thickness of the homogeneous films is 5 nm.

If the grating is surrounded by two homogeneous metal films, the model will be very close to the model of the metal composite film, described above. However, there are two differences. One is of major importance – in the grating, the embedded cylinders are not randomly distributed but organized in a periodic structure. The other is related to calculation simplifications and reflects the fact that in the first model the cylinders are circular, and in the second they are square.

3. Computational procedures

Set of codes has been developed for calculation of modes. The sums are truncated when the machine precision or saturation is reached. The poles of $\{a_n, b_n\}$ are found automatically by a special program. Conventional Lorenz-Mie calculations show that resonances (sharp minima/maxima) in the internal and scattered fields are related to the poles of the expansion coefficients $\{a_n, b_n\}$. Spectral peak positions depend on the size of particle, its shape and refractive index, and the refractive index of the surrounding medium [7]. In absorbing host matrix the particle extinction might have positive or negative values, as it follows from the optical theorem [8]. Thus, in the case of an absorbing host this decomposition of extinction into scattering and absorption is not possible because these two quantities are intrinsically positive. Our numeric simulations relate the range of wavelengths where extinction has a negative minimum, to the location of the enhanced transmission through the metal nanocomposite film by the use of effective refractive index for the composite film [4, 8].

The transmittance of the composite film is evaluated by the help of the slab effective refractive index N_{eff} :

$$N_{\text{eff}} = N_{\text{metal}} \frac{1 + i \pi f S(0)/k^3 v_p}{1 - i \pi f S(0)/k^3 v_p},$$

where $S(0)$ is the amplitude scattered by a particle in the forward direction, v_p is the sphere volume and f is the filling factor (ratio of v_p to sample volume) [5, 7]. Here we do not use the effective medium approximation, which is valid for small particles and low permittivity contrast (dipole approximation), but make use of the scattering matrix of an individual particle [7, 9]. This is the way N_{eff} is evaluated in scattering physics. In fact, that is the only approximation in our calculations.

Grating diffraction efficiencies are calculated in transmission and reflection for transverse electric (TE) and

transverse magnetic (TM) light polarization at normal incidence. The numeric analysis is based on the solution of the exact vector Maxwell's equations for diffractive and/or periodic structures. Algorithms for calculations use the transfer matrix method, which is equivalent to the rigorous multiwave coupled waves approach.

4. Results and discussion

4.1. Homogeneous spherical particles

In this section we give the main results of our model simulations and present some typical graphical illustrations. First of all, on the basis of the experimental data for the complex refractive index of silver [6], we have estimated some excitation characteristics of the metal matrix. The bulk plasmon frequency is at 3.81 eV (325.4 nm). The surface plasmon at the interface air – silver is located at 337 nm. All the resonance structures of the composite metal film with dielectric nanosized spheres have a considerable red shift from these plasmon wavelengths. In Fig. 1 we present the dispersion of the volume extinction efficiency C_v and the volume scattering efficiency S_v for a sphere with $N_p = 1.5$ and $r = 70$ nm. C_v has a maximum of 2.6 nm^{-1} at 392.6 nm, followed by a steep decrease to a minimum of -2.9 nm^{-1} at 397 nm. C_v is zero at 395 nm. The volume scattering efficiency S_v has a maximum at 395 nm and strength of 7500 nm^{-1} . There is a striking similarity of C_v and S_v normalized wavelength dependence, presented in Fig. 1, to the Kramers - Kronig relation between real and imaginary parts of a physical variable. In fact, the particle extinction is sum of the real parts of the electromagnetic mode coefficients (with appropriate weights), while the scattering is the sum of their absolute values.

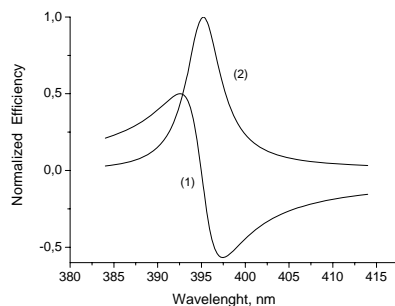


Fig. 1. Efficiency wavelength dependence for a sphere in Ag host matrix. $N_p = 1.5$ and $r = 70$ nm. Volume extinction efficiency C_v (1) and volume scattering efficiency S_v (2).

The main trends in the C_v dependence on particle radius and refractive index are as follows. With increase of the radius, the C_v structure is red shifted and its width diminishes (resonances are sharper). For $r > 100$ nm secondary resonances are observed in the blue part of the spectrum but their strengths are several orders of magnitude smaller. The increase of the refractive index from 1 to 1.74 (at a fixed sphere radius) reveals the same

trend: resonances are red shifted with N_p and become sharper. For spherical voids in Ag matrix ($N_p = 1$, $r = 70$ nm) the extinction minimum is at 344 nm.

Next, the wavelength dependence of the first terms of the complex $\{a_n, b_n\}$ modes are shown (Figures 2 and 3). Only the first ($n=1$) mode may be in resonance within the range of our model calculations. The remaining terms $\{a_n, b_n\}$ for $n>1$ are much smaller. Thus, the minimax structure in C_v is the result of the behavior of a single mode and has either dipole electric or dipole magnetic (eddy current) origin. The dipole mode real parts change sign at the resonance (Fig. 2 a) and 3 a)), while the imaginary parts have near Lorentzian shape, and can be either positive or negative (Figure 2 b) and 3 b)). For very small particles ($r < 20$ nm), in the wavelength region of interest, no mode is in resonance. For large particles ($r > 100$ nm) secondary structures appear at in the 360 – 380 nm range ($N_p = 1.5$), which are blue shifted from the main resonance. It is important to note that in this case the contribution from the magnetic dipole b_1 is predominant (Figure 4). Also, the character of the extinction dispersion is changed. For a sphere of $r = 150$ nm and $N_p = 1.5$, C_v passes through a minimum at 371.7 nm, a zero at 372.8 nm, and a maximum at 374 nm. For electric dipole resonance ($r = 70$ nm, $N_p = 1.5$) the zero of C_v is located at shorter wavelength than its minimum. Also, the scattering efficiency maximum is red shifted from the extinction minimum for magnetic mode resonance, while for electric dipole resonance it is blue shifted. This could help the identification of the character of the resonances in an eventual experimental situation. In general, the contribution of the magnetic modes is of major significance to the extinction process and cannot be ignored.

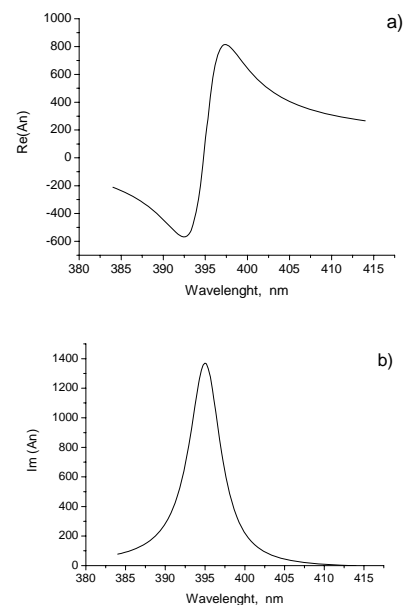


Fig. 2. Real – a) and Imaginary – b) parts of electric dipole mode a_1 . $N_p = 1.5$ and $r = 70$ nm.

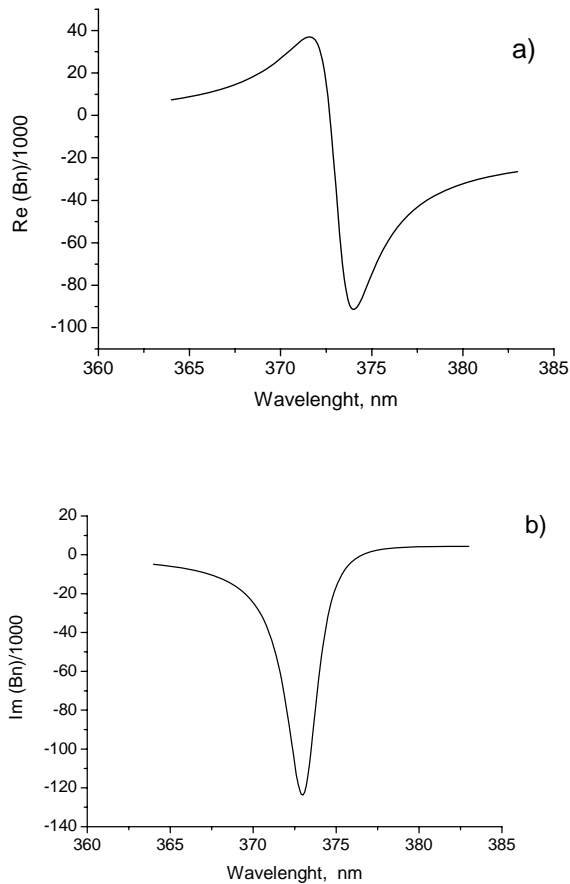


Fig. 3. Real part – a) and Imaginary part – b) of magnetic dipole mode b_1 , $N_p = 1.5$ and $r = 150$ nm.

4.2. Nanosized cylinders

In order to evaluate the effective refractive index of the nanosized composite film we first calculate the scattering amplitude matrix of a single dielectric circular cylinder in metal environment. The electric and magnetic modes are found in function of wavelength and light polarization. The $\{a_n, b_n\}$ coefficients are complex. Only the first ($n=1$) term is in resonance in the range of our model calculations. The remaining $\{a_n, b_n\}$ for $n>1$ are much smaller. At the resonance the modes imaginary parts have nearly Lorentzian shape. The modes real parts are of Fano type. In Figs. 1 and 2 we present the results for the real and imaginary part of the effective refractive index for values of the filling factor $f = 0.001; 0.005; 0.008$ and 0.01 and compare it to the complex refractive index of Au – curve 1 in both figures.

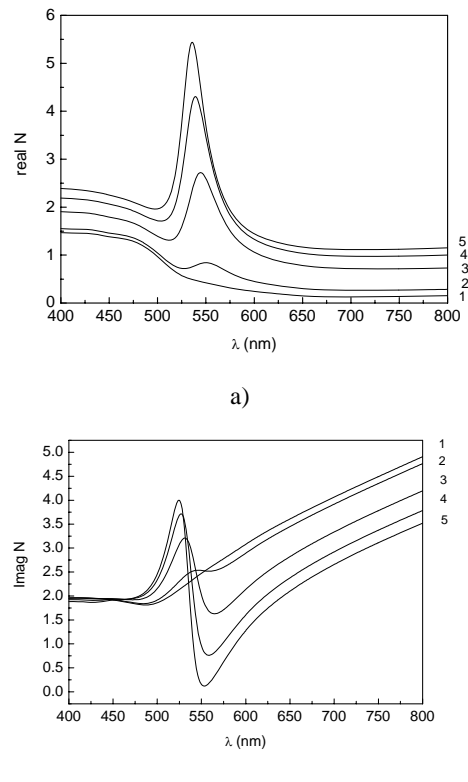


Fig. 4. Real – a) part and Imaginary – b) part of the film effective refractive index with different filling factor f : 1) – $f = 0$, 2) – $f = 0.001$; 3) – $f = 0.005$; 4) – $f = 0.008$; 5) – $f = 0.01$.

Results only for TM polarization are presented, the TE polarization shows no resonant structure. The resonance is at 550 nm, where there is a strong decrease of the absorption coefficient. Physically that means that the extinction cross section of particle has deep negative minimum and the composite film transmits more light. The low values of the filling factor assure that there is no multiple scattering between particles. The spectral transmission of the composite film is also calculated. The ET spectral position corresponds to the excitation of localized surface plasmon. Since the localized SPPs are confined to a volume roughness (topological defect) it results in a strong electromagnetic field enhancement at the particle/matrix interface. In the extreme case the dielectric particles can be considered as voids in the bulk of the metal. For the infinite cylinders the excitations share the properties of localized and propagating SPPs along the particle axis direction. In the case of mono dispersed scatterers (all particles have same shape and dimensions), the forward scattering is coherent and the resulting field amplitude of N particles is increased N^2 times. Other trends observed in the numeric simulations relate the size and the refractive index of the nanosized cylinders to the film optical response – increase of these parameters results in red shift of the transmission peak.

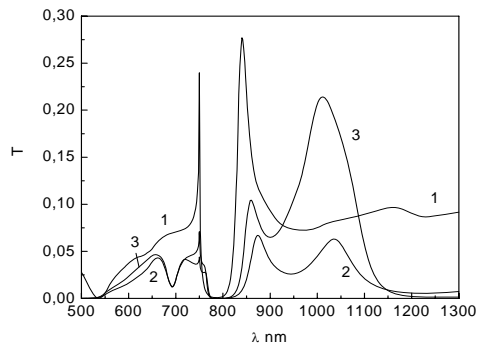


Fig. 5. Zero order diffraction of plasmonic crystal structure (see text for details).

Results from numeric simulation of plasmonic crystal structures described above in 2.2 are presented in Fig. 5. Only the case of TM polarization is presented because there is no transmission enhancement for TE polarization. Transmission at normal incidence (zero diffraction order) from the grating with no homogeneous layers is given as curve 1. The case of a plasmonic crystal, which consists of five crystal layers (five-‘unit cell’ of 5 gratings and 5 homogeneous layers) is also considered, curve 2. Curve 3 shows the zero diffraction order of the plasmonic crystal of 5 ‘unit cells’ plus one more homogeneous metal layer, placed at the top of the stack. This layer breaks the translation symmetry of the crystal but forms mirror symmetry and the overall structure has a pronounced interference character of Fabry-Perot type. The Wood’s anomaly related to the extinction of propagating diffraction orders is easily identified at 750 nm. Above this wavelength only one mode propagates and that is the zero order (directly transmitted light). A photonic band gap (no propagating light) is formed up to the wavelength of enhanced transmission at 820 nm. The 5-unit cell structure shows two transmission maxima of 5% each situated at 860 and 1040 nm. The situation is drastically changed when the addition layer embeds all cylinders (curve 3). The long wavelength maximum is increased up to 20% and it is slightly blue shifted. There is a small increase of the other maxima as well. The plasmonic stack maxima have larger half bandwidths, compared to the strictly periodic case. In periodic structures SPPs are excited at each metal-dielectric interface and they are propagating along both sides of each homogeneous dielectric layer. More, there is a strong interaction between SPPs on opposite film interfaces, if the film is sufficiently thin. This coupling results in the formation of forbidden zones (gaps) with enhanced suppression of transmission. ET is observed when SPPs become radiative by scattering with necessary wave vectors supplied by the periodic structure.

The optical behavior of the crystal stack correlates to the response of the composite film: both show strong light polarization selectivity; ET of resonant nature is formed; transmission maximum values increase when the dielectric fraction in the film/grating gets larger; there is a red shift of the ET with the increase of the refractive index of the

dielectric; under resonant condition transmission can be enhanced or suppressed; etc. In fact, the optical responses of the two structures are well described within the frame of classical electrodynamics by numerically calculating the scattering matrix of the composite film or the grating. The ET features can be analyzed by identifying its poles. Thus, the essential difference of the random and periodic structures is transferred into different mathematical methods for solution of the Maxwell’s equations. However, this approach does not reveal the conditions for the existence of resonant spectral structures.

In another series of simulations we have considered binary 2D subwavelength gratings with two periods of 500 nm and thickness of 40 to 140 nm. As for the cases described above, the grating is sandwiched between two homogeneous films. The sections of the dielectric parts of the gratings are 250×250 nm. The presence of the ‘symmetricising’ homogeneous films shifts the resonant peak to longer wavelengths and its HBW is enlarged. This structure is the photonic crystal analogue to the embedded dielectric particles (spheres) in metal host matrix, described above. Interplaying with the number of gratings and homogeneous layers in the photonic stack, and introducing different metals for the homogeneous films, we expected more pronounced changes in the ET, especially if the predominant mechanism is assumed to be related to the excitation and propagation of SPPs. It is well known that surface plasmons are exceptionally sensitive to the material environment [9]. However, we observed rather smooth changes in transmission. Without being conclusive evidence, we are inclined to accept M. M. Treacy point of view [12] for the nature of ET. He argues that dynamical diffraction theory can explain entirely the phenomenon of enhanced transmission. Surface plasmons are an integral part of the diffracted wave field and do not play “an active role” in transmitting and focusing of light.

5. Conclusions

We have developed accurate and flexible routines for evaluation of the electric and magnetic modes of dielectric spheres in metal host matrix. The pole locations of the modes are closely related to physical phenomena within the particles or in their immediate vicinity. As a result, after a resonant illumination of a nanosized composite structure of the kind discussed above, an enhancement of the near-field and far-field signals takes place. For particles with radius less than 150 nm, a particular peak in the wavelength spectrum is result of the behavior of a single mode. In the same time, the peak location is a sensitive function of the morphology of the particle (shape, size and refractive index) and the host matrix complex refractive index.

We have also analyzed the far-field optical response of plasmonic crystal structures and plasmonic amorphous composite films. Their optical behavior has common features that strongly correlate, i.e. the strong increase of the electromagnetic near-field, sensitivity to light polarization, resonant enhancement of transmission, dependence on period/film filling factors, etc.

The physical mechanisms of the considered models are related to surface plasmon polaritons excitations. In the periodic structures they are propagating modes that can (after excitation) be scattered back to light and thus contribute to the transmission enhancement. In the metal nanosized films the excited SPPs are localized. In absorbing host matrix at certain conditions the particle optical response shows negative extinction as a result of the behavior of a single electric or magnetic mode. The forward scattering of individual dielectric particles (or voids) is strictly constructively coherent. Thus the far-field transmitted signal will be enhanced due to the particle morphology dependent resonances. These resonances can be manipulated and engineered for novel applications in nanotechnologies, but this is one of the pictures, describing the process. ET nature might be related to SPPs excitations, but this can be also a matter of semantics.

References

- [1] T. Ebbesen, H. J. Lezec, H. F. Ghaemi, T. Thio, P. Wolff, *Nature (London)* **391**, 667 (1998).
- [2] W. Barnes, W. Murray, J. Dintinger, E. Devaux, T. Ebbesen, *Phys. Rev. B* **92**, 107401 (2004).
- [3] E. Popov, S. Enoch, G. Tayeb, M. Neviere, B. Gralak, N. Bonod, *Appl. Opt.* **43**, 999 (2004).
- [4] P. Sharlandjiev, D. Nazarova, B. Mednikarov, M. Pham, *Jour. Optoelectron. Adv. Mater.* **7**(1), 309 (2005).
- [5] A. Zayats, I. Smolyaninov, A. Maradudin, *Phys. Rep.*, **408**, 131 (2005).
- [6] P. B. Johnson, R. W. Christy, *Phys. Rev. B* **6**, 4370 (1972).
- [7] C. F. Bohren, D. R. Huffman, *Absorption and Scattering of Light by Small Particles*, John Wiley & Sons, New York (1983).
- [8] C. Bohren, D. Gilra, *J. Coll. Interf. Sci.* **72**, 215 (1972).
- [9] U. Kreibig, M. Vollmer, *Optical Properties of Metal Clusters*, Springer-Verlag, Berlin (1995).
- [10] P. Sharlandjiev, D. Nazarova, *Nanoscience & Nanotechnology*, **5**, 23, Heron Press, Sofia, (2005).
- [11] P. Sharlandjiev, D. Nazarova, *Nanoscience & Nanotechnology*, **6**, Heron Press, Sofia, (2006).
- [12] M. M. Treacy, *Phys. Rev B*, **66**, 195105 (2002).

*Corresponding author: dimana@optics.bas.bg